INSTITUT DE FRANCE
Académie des sciences

# Comptes Rendus
# Mécanique

Daniel Dorostghoal, Abdolreza Zare and Ali Alipour Mansourkhani

**Exact free vibration of symmetric three-layered curved sandwich beams using dynamic stiffness matrix**

Volume 348, issue 5 (2020), p. 375-392

Published online: 10 November 2020

https://doi.org/10.5802/crmeca.45

This article is licensed under the
Creative Commons Attribution 4.0 International License.
http://creativecommons.org/licenses/by/4.0/

*Les* Comptes Rendus. Mécanique *sont membres du Centre Mersenne pour l'édition scientifique ouverte*
www.centre-mersenne.org
e-ISSN : 1873-7234

*Comptes Rendus*
*Mécanique*
**2020**, 348, nº 5, p. 375-392
https://doi.org/10.5802/crmeca.45

# Exact free vibration of symmetric three-layered curved sandwich beams using dynamic stiffness matrix

**Daniel Dorostghoal**[*, a], **Abdolreza Zare**[a] **and Ali Alipour Mansourkhani**[a]

[a] Department of Civil Engineering, Yasouj University, Yasouj, Iran

*E-mails:* ddorostghoal@yahoo.com (D. Dorostghoal), zare@yu.ac.ir (A. Zare), aalipourm@yu.ac.ir (A. Alipour Mansourkhani)

**Abstract.** In the present study, the governing differential equations of motion are developed by using the Hamilton principle for a three-layered curved sandwich beam with symmetric face layers. To develop the dynamic stiffness matrix, the face layers are considered to behave like Euler–Bernoulli beams although only shear deformation occurs in the core. In this research, for computing the natural frequencies of curved sandwich beams, the Wittrick–Williams algorithm is applied. After the procedure is validated by comparison with various published results, to indicate its range of application, natural frequencies of a complex frame are computed. Finally, a parametric study investigated the effect of thickness and curvature for various boundary conditions on the natural frequencies.

**Keywords.** Free vibration, Curved sandwich beam, Wittrick–Williams algorithm, Exact dynamic stiffness matrix, Natural frequency.

*Manuscript received 22nd October 2019, revised 28th July 2020, accepted 7th September 2020.*

## 1. Introduction

Sandwich beams are used extensively in a variety of industries due to their unique features such as high strength-to-weight ratio, good buckling resistance, high specific stiffness, formability into complex shapes, and easy reparability. Moreover, these structures are used widely, for example, in aircraft, automobile, and marine applications, which are weight-sensitive industries [1]. Accordingly, many researchers have investigated the free vibration of sandwich beams. Di Taranto [2], Mead and Sivakumaran [3], and Mead and Marcus [4] are pioneering researchers who solved the governing differential equations of motion by using the classical theory and investigated the free vibration of sandwich beams by calculating mode shapes and natural frequencies. The free vibration of curved sandwich beams was studied by Ahmed [5, 6] by using the finite element procedure. He also investigated the effect of parameters such as curvature, core rigidity, core-to-face thickness ratio, and core-to-face density ratio on the natural frequencies of curved sandwich

* Corresponding author.

beams. Sakiyama *et al.* [7] studied the effects of several types of boundary conditions on the free vibration of a three-layered arch with various axis shapes by using an analytical method. They used the Green function for deriving the free vibration characteristic equation and evaluated the effects of core thickness, shear modulus, and a viscoelastic or elastic core on the natural frequency. A higher order refined model was presented by Marur and Kant [8] by considering seven degrees of freedom per node based on the expansion of Taylor's series and finite element modeling to analyze the free vibration of composite and sandwich arches. By using the penalty method to impose boundary condition and material discontinuity, Amirani *et al.* [9] calculated the natural frequencies of a sandwich beam with functionally graded core by applying the Galerkin method as a meshless method. Hashemi and Adique [10] used the dynamic finite element method to study the free vibration of sandwich beams with symmetric face layers by applying the method of weighted residuals to develop the governing equations. They assumed that the face layers follow the Euler–Bernoulli theory, whereas the core undergoes shear deformation only. In subsequent work, Hashemi and Adique [11] developed the previous model and considered the Timoshenko beam theory for the core's behavior, while the Rayleigh beam theory was followed for the face layers to investigate the free vibration of three-layered sandwich beams. Composite sandwich beam consists of a viscoelastic core studied via a higher order theory by Arvin *et al.* [12]. They assumed independent transverse displacements in face layers with linear variations through the core's depth and showed that when the face layer fiber angles, thickness of the core, or both increase, the natural frequencies for soft core beam decrease. By applying the finite element and dynamic stiffness methods, the free vibration analysis of a sandwich beam with symmetric face layers was reviewed by Khalili *et al.* [13]. Their results revealed that irrespective of the boundary condition type, when the core-to-face density ratio increases, the first natural frequency decreases, whereas this frequency increases when the shear modulus of the core and the face-to-core thickness ratio increase. Khdeir and Aldraihem [1] presented a new zigzag beam theory to carry out research on the free vibration of soft-core sandwich beams. They used the state-space method to solve for the mode shapes and natural frequencies of sandwich beams. They also investigated the effects of core thickness and length/thickness ratio on the frequency for various boundary conditions. Sadeghpour *et al.* [14] analyzed the debonding effect on frequencies of a curved sandwich beam. They applied with-contact and without-contact linear models to the debonded area by developing a high-order theory and analyzed the effects of the boundary condition and the curvature angle on the vibration of a curved sandwich beam. Chen *et al.* [15] studied a shear-deformable sandwich porous core beam and the effects of parameters including slenderness ratio, coefficient of porosity, thickness ratio, varying porosity distributions, and boundary conditions on the nonlinear free vibration of this beam. Many researchers have used the dynamic stiffness matrix method to analyze the free vibration of structural elements, including Banerjee's research as one of the pioneering studies on this method. He used the dynamic stiffness method as a general theory, which saves computation time compared to numerical methods, to compute the natural frequencies of a structure [16]. Using the dynamic stiffness method, Banerjee [17] studied the free vibration analysis of three-layered symmetric sandwich beams in which the Euler–Bernoulli beam model is considered for face layers and only transverse shear occurs in the core. Banerjee [18] analyzed the free vibration of a twisted Timoshenko beam by developing an exact dynamic stiffness matrix. He studied the effects of shear deformation and rotational inertia on natural frequencies and showed that the effects on the natural frequencies of a twisted beam are similar to those of an untwisted beam. Banerjee and Sobey [19] developed Banerjee's previous model [17]. They assumed that the faceplates behave like a Rayleigh beam while the core is modeled as a Timoshenko beam. By solving the governing differential equation through closed form, Howson and Zare [20] presented an exact dynamic stiffness matrix to study the flexural vibration of a sandwich beam having unequal faceplates, which necessitated the so-

lution of a transcendental eigenvalue problem. Unlike the finite element method wherein the idealization affects the accuracy, this technique enables the convergence on any required natural frequency with certainty. The difference between the studies by Howson and Zare [20] and Banerjee [17] was that Banerjee [17] assumed that the core mass versus the face mass is negligible while Howson and Zare [20] derived the equations of motion without considering the axial acceleration of the beam and by taking into account the bending acceleration of the beam along with the core mass. In subsequent work, Banerjee *et al.* [21] idealized all layers of the sandwich beam, and the Timoshenko beam theory was considered for each layer; their results were compared with the previous work by Banerjee and Sobey [19]. Banerjee and Gunawardana [22] investigated the effects of moving speed and axial load on the free vibration characteristics of a moving Euler–Bernoulli beam by applying the dynamic stiffness method. Damanpack and Khalili [23] utilized the dynamic stiffness method to investigate the high order free vibration of sandwich beams with a flexible core. Mode shapes and natural frequencies were calculated by applying numerical techniques and the Wittrick–Williams algorithm [24], and the results were compared with experimental results. Su *et al.* [25] analyzed the free vibration behavior of functionally graded beams using the dynamic stiffness method derived from the Euler–Bernoulli theory. They supposed that the properties of material varied continuously in the thickness direction of the beam in accordance with a power law distribution and showed that by considering these assumptions, modal interchange between axial and bending modes and vice versa might take place. Pagani *et al.* [26] used the Carrera unified formulation and the dynamic stiffness method to study the free vibration of laminated composite beams with arbitrary boundary conditions. Banerjee and Jackson [27] and Banerjee and Kennedy [28] investigated the effect of rotational speed on the natural frequencies of rotating beams' free vibration by utilizing the dynamic stiffness method. In subsequent work, Su and Banerjee [29] developed a dynamic stiffness matrix to study the effects of length-to-thickness ratio and material distribution on mode shapes and natural frequencies of functionally graded Timoshenko beams. Zare *et al.* [30] studied coupled bending–longitudinal vibrations of three-layered sandwich beams by using the exact dynamic stiffness matrix. They showed that except for some unusual states, for any structure constructed from sandwich elements, three families of modes—flexural, axial, and shear thickness—are expected. However, no one appeared to have applied a formulation of exact dynamic stiffness for the free vibration of curved sandwich beams to consider uniform mass distribution in a member. The current paper focuses on this subject. The dynamic stiffness method has several advantages compared with the finite element method and other approximate methods [31, 32]. For example, the exact formulation leads to an idealization consisting of the minimum number of elements. Another considerable advantage is that the dynamic stiffness matrix of an element depends only on the frequency accounts for both stiffness and mass properties. Therefore, as in the finite element method, the dynamic stiffness matrices of all single elements in a structure can be assembled. In the present study, first, by utilizing the Hamilton principle, the governing equations of motion are presented. Then, after imposing harmonic oscillations, two partial differential equations are written in the form of a sixth-order governing differential equation whose closed-form solution is developed into an exact dynamic member stiffness matrix of a curved sandwich beam. To calculate the natural frequencies of explanatory examples taken from the literature, the Wittrick–Williams [24] algorithm is used.

## 2. Theory

To form the dynamic stiffness matrix of a three-layered curved sandwich beam, it is presumed that throughout the thickness, the transverse displacement doesn't vary, the faces are elastic and homogeneous and the shear within them is zero, the homogeneous orthotropic core is rigid in the $z$-direction and carries only shear, and there is perfect bonding between interfaces of layers.

The beam length is denoted by $L$ and the radius at the mid-plane of the beam is denoted by $R$. The beam has unit width, and $t$ is the thickness of the outer and inner faces while $t_c$ is the core thickness. The $z$-axis represents the normal coordinate, and it starts from the middle surface of every layer; the $y$-axis represents the circumferential coordinate, and it is located at the center line of the curved beam. The faceplates are modeled as Euler–Bernoulli beams, while only shear deformation exists in the core and beam deflections occur only in the $y$–$z$ plane. The parameter $w$ is the radial displacement, which remains constant for all the layers, and $v_1$ and $v_2$ are the circumferential displacements of the interior and exterior layers, respectively. Figure 1 shows the coordinate system for a curved sandwich beam with symmetric face layers. The relations of displacement–strain can then be written as [5]

$$\varepsilon_{yi} = \frac{\partial v_1}{\partial y} + \frac{w}{R} - z\frac{\partial^2 w}{\partial y^2}; \quad \varepsilon_{yo} = \frac{\partial v_2}{\partial y} + \frac{w}{R} - z\frac{\partial^2 w}{\partial y^2}; \quad \varepsilon_c = \frac{\varepsilon_z}{1+\frac{z}{R}}, \tag{1}$$

where $\varepsilon_{yi}, \varepsilon_{yo}$, and $\varepsilon_c$ are the interior face total strain, exterior face total strain, and core total strain, respectively, $z$ is the normal coordinate starting from the middle surface of every layer, and

$$\varepsilon_z = \frac{1}{t_c}\left[\left(1-\frac{t_c}{2R}\right)v_2 - \left(1+\frac{t_c}{2R}\right)v_1 + h\frac{\partial w}{\partial y}\right]; \quad h = t + t_c. \tag{2}$$

As we only consider the flexural vibration,

$$v_1 = -v_2 = -v. \tag{3}$$

The parameter $U$ is the potential energy of a curved sandwich beam with three layers. It consists of three parts. They are the strain energy of the top and bottom faces, $U_{of}$ and $U_{if}$, respectively, and the strain energy of the core, $U_c$:

$$U = U_{if} + U_{of} + U_c. \tag{4}$$

Since the beam has unit width, we have

$$U_{if} = \frac{1}{2}\int_0^L \int_{-\frac{t}{2}}^{\frac{t}{2}} \sigma_{fi}\,\varepsilon_{yi}\,\mathrm{d}z\,\mathrm{d}y, \tag{5}$$

$$U_{of} = \frac{1}{2}\int_0^L \int_{-\frac{t}{2}}^{\frac{t}{2}} \sigma_{fo}\,\varepsilon_{yo}\,\mathrm{d}z\,\mathrm{d}y, \tag{6}$$

$$U_c = \frac{1}{2}\int_0^L \int_{-\frac{t_c}{2}}^{\frac{t_c}{2}} \sigma_c\varepsilon_c\,\mathrm{d}z\,\mathrm{d}y, \tag{7}$$

where by using (1), we have

$$\sigma_{fi} = E\varepsilon_{yi}; \quad \sigma_{fo} = E\varepsilon_{yo}; \quad \sigma_c = G_c\varepsilon_c. \tag{8a,b,c}$$

Here, $\sigma_{fi}$, $\sigma_{fo}$, and $\sigma_c$ are the normal stresses on the inner and outer faces and the core transverse shear stress, respectively; $E$ and $G_c$ are the elasticity modulus and core shear modulus, respectively.

The total kinetic energy of the curved beam denoted by $T$ consists of three parts, the kinetic energy of two faces, $T_{if}$ and $T_{of}$, and the kinetic energy for the core $T_c$:

$$T = T_{if} + T_{of} + T_c, \tag{9}$$

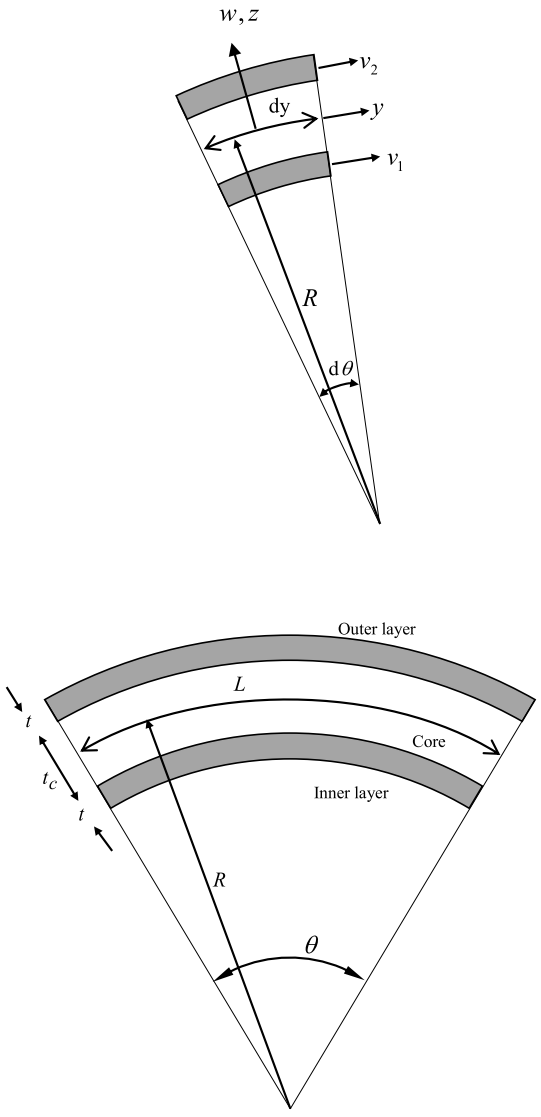


**Figure 1.** Symmetric three-layered curved sandwich beam and its coordinate system: (a) infinitesimal element and the coordinate system; (b) beam configuration.

where

$$T_{if} = \frac{1}{2}\rho_f \int_0^L \int_{-\frac{t}{2}}^{\frac{t}{2}} \left[\dot{v}_1^2 + \dot{w}^2\right] \mathrm{d}z\,\mathrm{d}y, \tag{10}$$

$$T_{of} = \frac{1}{2}\rho_f \int_0^L \int_{-\frac{t}{2}}^{\frac{t}{2}} \left[\dot{v}_2^2 + \dot{w}^2\right] \mathrm{d}z\,\mathrm{d}y, \tag{11}$$

$$T_c = \frac{1}{2}\rho_c \int_0^L \int_{-\frac{t_c}{2}}^{\frac{t_c}{2}} \left[\dot{v}_c^2 + \dot{w}^2\right] \mathrm{d}z\,\mathrm{d}y. \tag{12}$$

Here, $\rho_f$ and $\rho_c$ are the mass per unit volume of the two faces and the core, respectively, and $v_c$ is the core's circumferential displacement defined by

$$v_c = -\frac{z}{t_c}\left[(v_1 - v_2) - t\frac{\partial w}{\partial y}\right]. \tag{13}$$

The dot and prime in expressions indicate differentiation with respect to time and $y$.

The Hamilton principle states that in a conservative system, equations of motion are obtained from the first time variation of the difference between potential and kinetic energies in any interval of time with respect to all independent variables of the system, that is,

$$\delta^{(1)}\varphi = \delta^{(1)}\int_{t_1}^{t_2}(U-T)\,\mathrm{d}t = \delta^{(1)}\int_{t_1}^{t_2}\int_0^L F\,\mathrm{d}y\,\mathrm{d}t = 0. \tag{14}$$

The function $F$ can then be obtained using (4) and (9):

$$F = \frac{1}{2}\left\{\alpha_1^2\left[v'^2 + \left(\frac{w}{R}\right)^2\right] + \alpha_3^2 w''^2 + \alpha_2^2\left(2v + h\,w'\right)^2 - \left(\beta\dot{v}^2 + \gamma\dot{w}^2\right)\right\}, \tag{15}$$

where

$$\alpha_1 = \sqrt{2Et};\quad \alpha_2 = \sqrt{\left(\frac{1}{t_c} + \frac{t_c}{4R^2}\right)G_c} \tag{16a}$$

$$\alpha_3 = \sqrt{\frac{Et^3}{6}};\quad \beta = 2t\rho_f + \tfrac{1}{3}t_c\rho_c;\quad \gamma = 2t\rho_f + t_c\rho_c. \tag{16b}$$

The Euler–Lagrange equations are generated from (14) as follows:

$$\frac{\partial F}{\partial v} - \frac{\partial}{\partial y}\frac{\partial F}{\partial v'} - \frac{\partial}{\partial t}\frac{\partial F}{\partial \dot{v}} = 0;\quad \frac{\partial F}{\partial w} - \frac{\partial}{\partial y}\frac{\partial F}{\partial w'} - \frac{\partial}{\partial t}\frac{\partial F}{\partial \dot{w}} + \frac{\partial^2}{\partial y^2}\frac{\partial F}{\partial w''} = 0. \tag{17a,b}$$

At the ends of the beam, the boundary conditions are

$$\begin{cases} \dfrac{\partial F}{\partial w''} = 0 \text{ or } w' = 0 \\ \dfrac{\partial}{\partial y}\dfrac{\partial F}{\partial w''} - \dfrac{\partial F}{\partial w'} = 0 \text{ or } w = 0 \\ \dfrac{\partial F}{\partial v'} = 0 \text{ or } v = 0. \end{cases} \tag{18a,b,c}$$

Now, imposing (17a,b) on (15) gives us the required partial differential equations of motion as follows:

$$\begin{cases} 4\alpha_2^2 v + 2h\alpha_2^2 w' - \alpha_1^2 v'' + \beta\ddot{v} = 0, \\ \dfrac{\alpha_1^2}{R^2}w - \alpha_2^2 h^2 w'' - 2h\alpha_2^2 v' + \gamma\ddot{w} + \alpha_3^2 w'''' = 0. \end{cases} \tag{19}$$

Relations for axial force, shear force, and bending moment are defined by applying the boundary conditions as follows:

$$\begin{cases} \alpha_1^2 v' = n = 0, \\ \alpha_3^2 w''' - \alpha_2^2 h^2 w' - 2\alpha_2^2 h v = q = 0, \\ \alpha_3^2 w'' = m = 0, \end{cases} \tag{20a,b,c}$$

where $n$, $q$, and $m$ are the axial force, the shear force, and the bending moment at the ends of the member, respectively.

Now, the effect of harmonic motion applies as follows:

$$f(y,t) = F(y)\,\mathrm{e}^{\mathrm{i}\omega t}. \tag{21}$$

Applying (21) to the partial differential equations of motion yields the following linear differential equations:

$$\begin{cases} -\dfrac{2h\alpha_2^2}{\alpha_1^2}W' + \dfrac{1}{\alpha_1^2}\left(\omega^2\beta - 4\alpha_2^2\right)V + V'' = 0, \\ \dfrac{1}{\alpha_3^2}\left(\dfrac{\alpha_1^2}{R^2} - \omega^2\gamma\right)W - \dfrac{h^2\alpha_2^2}{\alpha_3^2}W'' + W'''' - \dfrac{2h\alpha_2^2}{\alpha_3^2}V' = 0. \end{cases} \tag{22}$$

Furthermore, substituting (21) into (20), the other requirements for developing the required stiffness relation are

$$\begin{cases} \alpha_3^2 W'' = M, \\ \alpha_3^2 W''' - \alpha_2^2 h^2 W' - 2\alpha_2^2 hV = Q, \\ \alpha_1^2 V' = N. \end{cases} \tag{23}$$

Due to the appearance of $W'$ in boundary condition equations, we introduce

$$\psi = \frac{\mathrm{d}W}{\mathrm{d}y}, \tag{24}$$

and the matrix form of (22) is generated by employing the operator $D = \mathrm{d}/\mathrm{d}y$ as follows:

$$\begin{bmatrix} D^2 + \dfrac{1}{\alpha_1^2}\left(\omega^2\beta - 4\alpha_2^2\right) & -\dfrac{2h\alpha_2^2}{\alpha_1^2}D \\ -\dfrac{2h\alpha_2^2}{\alpha_3^2}D & D^4 + \dfrac{1}{\alpha_3^2}\left(\dfrac{\alpha_1^2}{R^2} - \omega^2\gamma\right) - \dfrac{h^2\alpha_2^2}{\alpha_3^2}D^2 \end{bmatrix} \begin{bmatrix} V \\ W \end{bmatrix} = 0. \tag{25}$$

The following sixth-order linear differential equation results via developing the determinant of the matrix operator:

$$\left[D^6 + c_1 D^4 + c_2 D^2 + c_3\right]\Phi = 0, \tag{26}$$

where

$$\begin{cases} c_1 = \dfrac{1}{\alpha_1^2}\left(\omega^2\beta - 4\alpha_2^2\right) - \dfrac{h^2\alpha_2^2}{\alpha_3^2}, \\ c_2 = \dfrac{1}{\alpha_3^2}\left(\dfrac{\alpha_1^2}{R^2} - \omega^2\gamma\right) - \dfrac{h^2\alpha_2^2\omega^2\beta}{\alpha_1^2\alpha_3^2}, \\ c_3 = \dfrac{1}{\alpha_1^2\alpha_3^2}\left(\omega^2\beta - 4\alpha_2^2\right)\left(\dfrac{\alpha_1^2}{R^2} - \omega^2\gamma\right), \end{cases} \tag{27}$$

and $\Phi$ can be either of the variables $V$ or $W$. The linear differential equation (Equation (26)) can be solved in the following form:

$$\Phi = \sum_{j=1}^{6} H_{ij} C_j \xi_j; \quad \xi_j = \mathrm{e}^{\eta_j y}; \quad 0 < y < L. \tag{28a,b}$$

Substituting (28b) into (26) yields the characteristic equation (Equation (29)) whose roots are $\eta_j$ and $C_j$ are arbitrary constants:

$$\eta^6 + c_1\eta^4 + c_2\eta^2 + c_3 = 0. \tag{29}$$

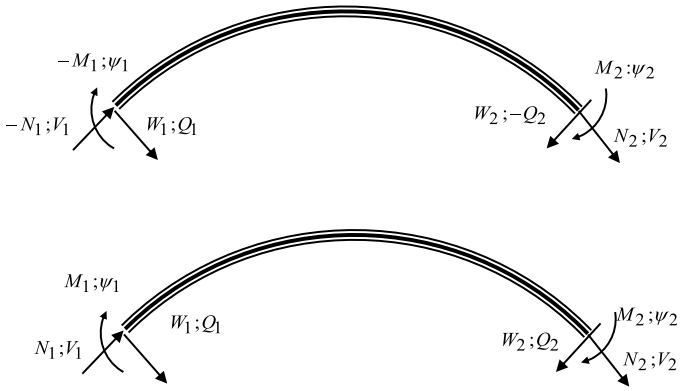


**Figure 2.** Nodal displacements and forces: (a) local coordinate system; (b) member coordinate system.

The $\eta_j$ define $\Phi$, and (23) and (24) are other required quantities for the stiffness formulation, which yield the following results:

$$W=\sum_{j=1}^{6} H_{1j}\,C_j\,\xi_j;\quad \psi=\sum_{j=1}^{6} H_{2j}\,C_j\,\xi_j;\quad V=\sum_{j=1}^{6} H_{3j}\,C_j\,\xi_j \tag{30a}$$

$$Q=\sum_{j=1}^{6} H_{4j}\,C_j\,\xi_j;\quad M=\sum_{j=1}^{6} H_{5j}\,C_j\,\xi_j;\quad N=\sum_{j=1}^{6} H_{6j}\,C_j\,\xi_j. \tag{30b}$$

It is assumed that $H_{1j}=1$; accordingly, relations between the $H_{ij}$ are obtained as follows:

$$H_{1j}=1,\quad H_{2j}=\eta_j,\quad H_{3j}=\frac{2h\alpha_2^2\eta_j}{\alpha_1^2\eta_j^2+\omega^2\beta-4\alpha_2^2} \tag{31a}$$

$$H_{4j}=\alpha_3^2\eta_j^3-\alpha_2^2h^2\eta_j-2h\alpha_2^2H_{3j},\quad H_{5j}=\alpha_3^2\eta_j^2,\quad H_{6j}=\alpha_1^2H_{3j}\eta_j. \tag{31b}$$

Now, to transform from the local coordinate system (Figure 2(a)) to the member coordinate system (Figure 2(b)), Equation (32) is imposed on (23) and (24):

$$\text{at}\quad y=0:\quad W=W_1,\quad \psi=\psi_1,\quad V=V_1,\quad Q=Q_1,\quad M=-M_1,\quad N=-N_1, \tag{32a}$$

$$\text{at}\quad y=L:\quad W=W_2,\quad \psi=\psi_2,\quad V=V_2,\quad Q=-Q_2,\quad M=M_2,\quad N=N_2, \tag{32b}$$

and from (30),

$$d=S\cdot C\quad\text{and}\quad p=S^*\cdot C, \tag{33}$$

where

$$d=\begin{bmatrix}W_1\\ \psi_1\\ V_1\\ W_2\\ \psi_2\\ V_2\end{bmatrix},\quad p=\begin{bmatrix}Q_1\\ M_1\\ N_1\\ Q_2\\ M_2\\ N_2\end{bmatrix},\quad C=\begin{bmatrix}C_1\\ C_2\\ C_3\\ C_4\\ C_5\\ C_6\end{bmatrix} \tag{34}$$

and

$$\begin{gathered}s_{1j}=H_{1j};\quad s_{2j}=H_{2j};\quad s_{3j}=H_{3j},\quad s_{4j}=H_{1j}\chi_j;\quad s_{5j}=H_{2j}\chi_j;\quad s_{6j}=H_{3j}\chi_j,\\ s_{1j}^*=H_{4j};\quad s_{2j}^*=-H_{5j};\quad s_{3j}^*=-H_{6j};\quad s_{4j}^*=-H_{4j}\chi_j;\quad s_{5j}^*=H_{5j}\chi_j;\quad s_{6j}^*=H_{6j}\chi_j,\\ \chi_j=\mathrm{e}^{\eta_jL}\quad(j=1,2,\ldots,6).\end{gathered} \tag{35}$$

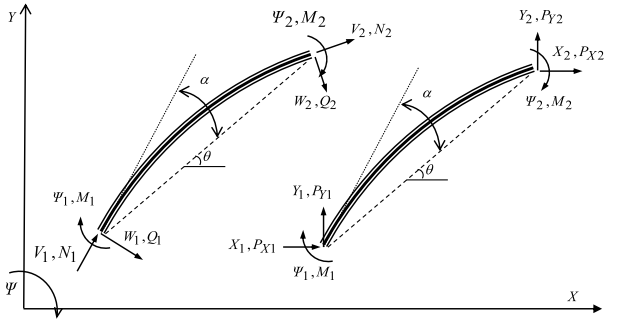


**Figure 3.** Nodal forces and displacements of a curved sandwich beam: (a) member coordinate system; (b) global coordinate system.

Here, $s_{ij}$ and $s^*_{ij}$ are the components of $S$ and $S^*$, respectively. In the following, by omitting the constant vector $C$ from (33), the required dynamic stiffness matrix $k$ can be produced:

$$C = S^{-1}d, \quad \text{so} \quad p = kd, \quad \text{where} \quad k = S^* \cdot S^{-1}. \tag{36}$$

## 3. Transformation matrix

To analyze the curved sandwich beam in a plane structure, stiffness matrix transformation from member coordinates to global coordinates is essential (see Figure 3). Moments and rotations during this process remain unchanged. Thus, from Figure 3, it is obvious that

$$\begin{cases} X_1 = W_1 \operatorname{Sin}(\theta+\alpha) + V_1 \operatorname{Cos}(\theta+\alpha) \\ Y_1 = -W_1 \operatorname{Cos}(\theta+\alpha) + V_1 \operatorname{Sin}(\theta+\alpha) \\ X_2 = W_2 \operatorname{Sin}(\theta-\alpha) + V_2 \operatorname{Cos}(\theta-\alpha) \\ Y_2 = -W_2 \operatorname{Cos}(\theta-\alpha) + V_2 \operatorname{Sin}(\theta-\alpha) \end{cases}, \quad \begin{cases} P_{X1} = Q_1 \operatorname{Sin}(\theta+\alpha) + N_1 \operatorname{Cos}(\theta+\alpha) \\ P_{Y1} = -Q_1 \operatorname{Cos}(\theta+\alpha) + N_1 \operatorname{Sin}(\theta+\alpha) \\ P_{X2} = Q_2 \operatorname{Sin}(\theta-\alpha) + N_2 \operatorname{Cos}(\theta-\alpha) \\ P_{Y2} = -Q_2 \operatorname{Cos}(\theta-\alpha) + N_2 \operatorname{Sin}(\theta-\alpha) \end{cases}. \tag{37}$$

Equation (37) are transformation relations, and their matrix forms are written as follows:

$$d_G = \begin{bmatrix} X_1 \\ \Psi_1 \\ Y_1 \\ X_2 \\ \Psi_2 \\ Y_2 \end{bmatrix} = T \begin{bmatrix} W_1 \\ \Psi_1 \\ V_1 \\ W_2 \\ \Psi_2 \\ V_2 \end{bmatrix} = T\,d, \quad p_G = \begin{bmatrix} P_{X1} \\ M_1 \\ P_{Y1} \\ P_{X2} \\ M_2 \\ P_{Y2} \end{bmatrix} = T \begin{bmatrix} Q_1 \\ M_1 \\ N_1 \\ Q_2 \\ M_2 \\ N_2 \end{bmatrix} = T\,p, \tag{38}$$

where quantities in global coordinates are specified by the subscript $G$.

$$T = \begin{bmatrix} \sin(\theta+\alpha) & 0 & \cos(\theta+\alpha) & 0 & 0 & 0 \\ 0 & 1 & 0 & 0 & 0 & 0 \\ -\cos(\theta+\alpha) & 0 & \sin(\theta+\alpha) & 0 & 0 & 0 \\ 0 & 0 & 0 & \sin(\theta-\alpha) & 0 & \cos(\theta-\alpha) \\ 0 & 0 & 0 & 0 & 1 & 0 \\ 0 & 0 & 0 & -\cos(\theta-\alpha) & 0 & \sin(\theta-\alpha) \end{bmatrix}, \tag{39}$$

where $T$ is the transformation matrix. Thus, the element stiffness matrix in global coordinates, $k_G$, is

$$k_G = T^T k\, T. \tag{40}$$

## 4. Convergence on natural frequencies

After transformation of the stiffness matrix from member coordinates to global coordinates, by assembling the element matrices, the dynamic structure stiffness matrix $K$ is generated. By solving the equation $KD = 0$, the required natural frequencies are obtained. In many cases, this process is carried out by computing the determinant of $K$ and equaling it to zero. However, when $K$ is produced using the exact member theory, the calculation of the dynamic stiffness matrix determinant and finding when its sign changes through zero, can miss roots. This is because in the exact dynamic stiffness matrix method, the determinant of $K$ is a complex, transcendental function of natural frequency. Moreover, a number of natural frequencies may be near or may coincide with each other, whereas other frequencies may exceptionally be related to $D = 0$. The Wittrick–Williams algorithm [24] completely overcomes this problem. This algorithm utilizes a unique procedure to compute any structure's natural frequency to any desired precision. Instead of calculating the natural frequencies of a structure, the Wittrick–Williams algorithm [24] estimates the frequencies that are lower than an arbitrarily chosen trial frequency. For details, readers can refer to the original paper.

## 5. Numerical results and discussion

In this section, first, the dynamic stiffness theory and the Wittrick–Williams algorithm [24] are used to calculate the natural frequencies of curved sandwich beams under different boundary conditions taken from the literature to prove the validity of the theory and demonstrate its range of application. In Example 4, only the results of the authors are given for a frame consisting of two curved beams and one straight beam as the other studies do not give the natural frequencies for this frame using other formulations and methods. The validation of the results of this example is conducted via comparison with the results obtained by ABAQUS. Finally, the effect of thickness and curvature for various boundary conditions on the natural frequencies is studied.

### 5.1. *Example 1*

The first example considers a simply supported curved sandwich beam with identical faceplates, having the material and geometric properties listed in Table 1.

The first five natural frequencies are computed by using one element in the analysis, and the comparative results for these natural frequencies are presented in Table 2.

To confirm the correctness of the assembling process for the dynamic stiffness and the utilization of the Wittrick–Williams method [24], Figure 4 shows the normalized mode shapes of the first three natural frequencies of Example 1 by splitting the beam into six elements. Since the bending rigidity is very small compared with the circumferential rigidity, the bending deformations dominate.

### 5.2. *Example 2*

In this example, a clamped–clamped beam having the material and geometric properties listed in Table 1 is considered. Table 3 presents the comparative results.

### 5.3. *Example 3*

The next problem considers a cantilever supported curved sandwich beam having the material and geometric properties listed in Table 1. Table 4 presents the comparative results. In this

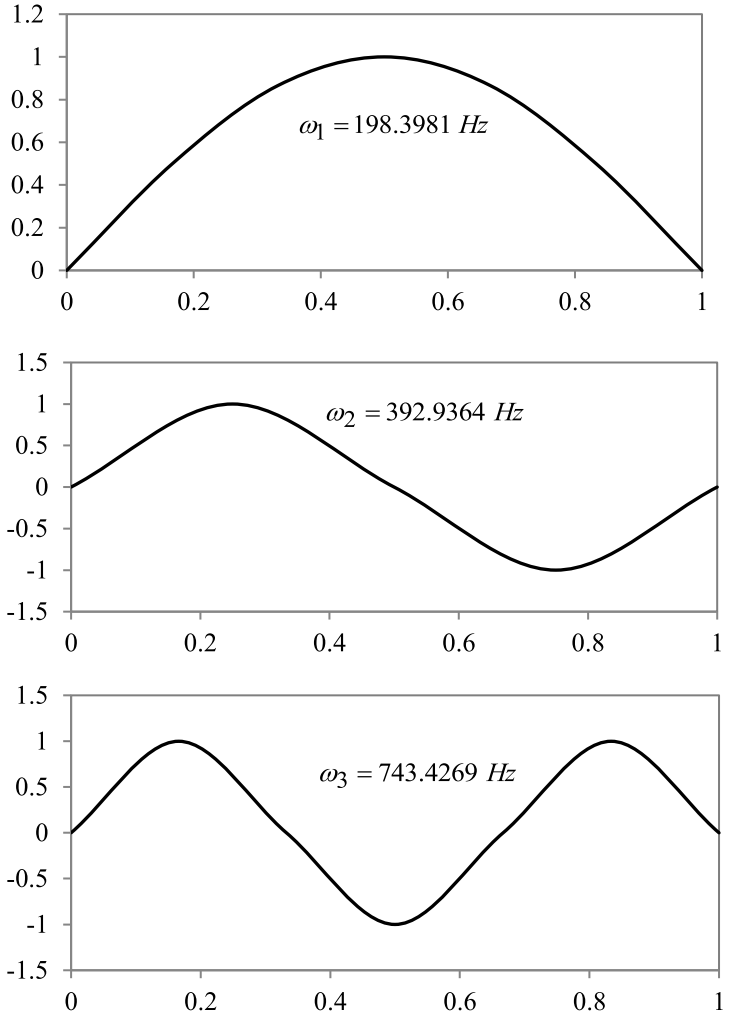


**Figure 4.** The normalized mode shapes corresponding to the first three natural frequencies of Example 1: first mode at 198.3981 Hz; second mode at 392.9364 Hz; third mode at 743.4269 Hz.

**Table 1.** Data for numerical examples

| Case | $L$ (m) | $t$ (mm) | $t_c$ (mm) | $E$ (GPa) | $R$ (m) | $\rho_f$ (kg·m$^{-3}$) | $\rho_c$ (kg·m$^{-3}$) | $G_c$ (MPa) |
|---|---|---|---|---|---|---|---|---|
| Material data | 0.7112 | 0.4572 | 12.7 | 68.9 | 4.2672 | 2680 | 32.8 | 82.68 |

example, there is a notable difference between the results of the current theory and the results obtained by Sakiyama *et al.* [7] and Marur and Kant [8] because of different basic assumptions and the consideration of transverse shear deformation. The ABAQUS results are also presented.

Tables 2–4 show good agreement between the results of the current theory and the available comparable results in the literature. The theory used by Ahmed [5] and Adique [33] is similar to the theory applied in the current study, that is, the transverse shear deformation is ignored. Therefore, their results have a very good correlation with the natural frequencies of the present theory. In the work by Ahmed [5, 34], the finite element method is used so that the degrees

**Table 2.** Natural frequencies (Hz) of simply supported curved sandwich beam

| Freq. No. | Current theory | Ahmed [5] | | Adique [33] | Sakiyama *et al.* [7] | Marur and Kant [8] |
|---|---|---|---|---|---|---|
| | | 7 elements | 10 elements | 40 elements | | |
| 1 | 198.3981 | 199.5 | 199.5 | 198.96 | 182.7 | 182.2877 |
| 2 | 392.9364 | 394 | 394 | 393.769 | 351.4 | 348.2241 |
| 3 | 743.4269 | 747 | 746 | 745.377 | 726.1 | 714.3247 |
| 4 | 1169.8081 | 1176 | 1175 | 1173.584 | 1162 | 1135.0752 |
| 5 | 1630.6193 | 1642 | 1639 | 1636.783 | 1633 | 1585.4760 |

**Table 3.** Natural frequencies (Hz) of clamped–clamped curved sandwich beam

| Freq. No. | Current theory | Ahmed [5] | | Adique [33] | Ahmed [34] | Marur and Kant [8] |
|---|---|---|---|---|---|---|
| | | 7 elements | 10 elements | 40 elements | 10 elements | |
| 1 | 262.0415 | 264.5 | 264.2 | 263.094 | 240 | 243.2431 |
| 2 | 515.4826 | 524 | 522 | 517.882 | 474 | 477.4111 |
| 3 | 871.4298 | 895 | 889 | 875.794 | 843 | 839.3961 |
| 4 | 1280.2359 | 1325 | 1312 | 1286.882 | 1253 | 1237.50 |
| 5 | 1719.0399 | 1792 | 1767 | 1728.185 | 1697 | 1664.37 |

**Table 4.** Natural frequencies (Hz) of cantilever curved sandwich beam

| Freq. No. | Current theory | Ahmed [5] | | Adique [33] | Sakiyama *et al.* [7] | Marur and Kant [8] | ABAQUS |
|---|---|---|---|---|---|---|---|
| | | 7 elements | 10 elements | 40 elements | | | |
| 1 | 178.0778 | 179 | 179 | 178.631 | 33.8 | 33.74 | 180.4352 |
| 2 | 264.6783 | 266 | 266 | 265.664 | 198.5 | 197.04 | 268.3472 |
| 3 | 540.3804 | 547 | 546 | 542.815 | 513 | 505.07 | 548.2974 |
| 4 | 921.8040 | 938 | 934 | 926.289 | 910 | 889.61 | 935.6445 |
| 5 | 1357.3238 | 1388 | 1379 | 1364.231 | 1356 | 1317.20 | 1378.01 |

of freedoms at each node, shape functions, and the number of elements affect the precision of results. Ahmed [5] studied a beam with four degrees of freedom per node and only flexural vibration, but in the next study [34], he used six degrees of freedom and the beam undergoes shear deformation. Therefore, due to less stiffness in the latter, the results are lower than those of the former. Adique [33] used the dynamic finite element method to analyze the free vibration of a symmetric curved sandwich beam based on Ahmed's theory [5]. As can be seen, by increasing the number of elements and consequently improving the accuracy of finite element methods, the required natural frequencies decrease. Since the present theory as an exact finite element method results in an idealization including the minimum number of elements, the results were expected to be lower than those obtained by Ahmed [5] and Adique [33]. Sakiyama *et al.* [7] derived the free vibration characteristic equation for a three-layered sandwich arch by employing Green functions, and Marur and Kant [8] analyzed the free vibration of sandwich arches with seven degrees of freedom per node using a higher order refined model. There are discrepancies between the results they obtained and those from the current study due to many factors including different basic assumptions, approximate solution methods, and the consideration of transverse shear deformation.

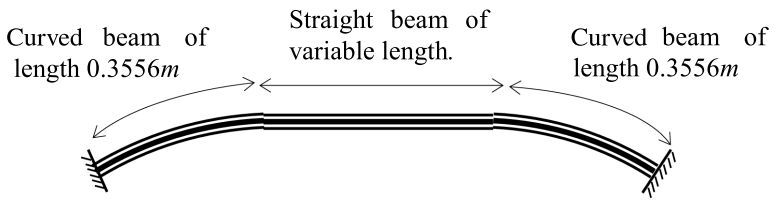


**Figure 5.** Frame of Example 4 consisting of two curved sandwich beams and one straight sandwich beam.

### 5.4. *Example 4*

To indicate the range of application of the current theory, a frame consisting of two curved beams and one straight beam with identical faceplates, shown in Figure 5, is analyzed. Since the formulations and methods by other authors cannot be used for this complex frame, Table 5 gives only the results of the current study. As regards the obtained frequencies not depending on the considered elements, the dynamic stiffness method is an accurate procedure. However, in the finite element method, the precision of results depends on the number of elements, which shows its effect at higher frequencies. As is seen in previous examples, at higher frequencies, the difference between the results of the dynamic stiffness matrix theory and the finite element method has increased. In the dynamic stiffness method, mass and stiffness effects are considered in the element's dynamic stiffness matrix that is only based on frequency. This makes it possible to assemble the individual element matrices of a structure in a common procedure.

In the present formulation, by considering $R$ equal to infinity in the formulations, the straight beam stiffness matrix can be generated. The basic material and geometric properties of curved and straight beams are the same as those listed in Table 1 except that the lengths of curved beams are 0.3556 m and various lengths are considered for straight beams. The lengths of straight beams are 0.4 m, 0.2 m, 0.05 m, and 0.001 m.

Table 5 presents the authors' results for a frame consisting of two curved beams and one straight beam with identical faceplates shown in Figure 5. Due to a lack of comparable frames in the literature, frequency validity is checked by comparing with the results of modeling in ABAQUS. From Table 5, it can be observed that there are no notable differences between the results obtained from the theory and ABAQUS. Furthermore, we used a parametric study to validate the results as follows. The results in column 2 of Table 5 were obtained using a straight beam of length 0.4 m. Then, the length of the straight beam was reduced gradually. By doing this, since the frame is clamped–clamped, the required natural frequencies should come close to the natural frequencies of the curved beam in Example 2. As can be seen in column 7 of Table 5, when the length of the straight beam is 0.001 m, the results are very close to the frequencies from Example 2.

### 5.5. *Parametric study of the free vibration analysis*

In this section, parametric studies are presented to analyze the effect of thickness and curvature on natural frequencies of sandwich beams for the case in Table 1.

The effect of variation in face/core thickness ratios on natural frequencies has been studied, and the results are given in Tables 6–8. In this case, the face thickness is considered constant, but the core thickness is varied. The ratio of face thickness to core thickness of the beam presented in Table 1 is $t/t_c = 0.036$. The variation in the first natural frequency with $t/t_c$ ratios is shown in Figure 6. As is obvious in Figure 6, when the face/core thickness ratio increases, the first natural

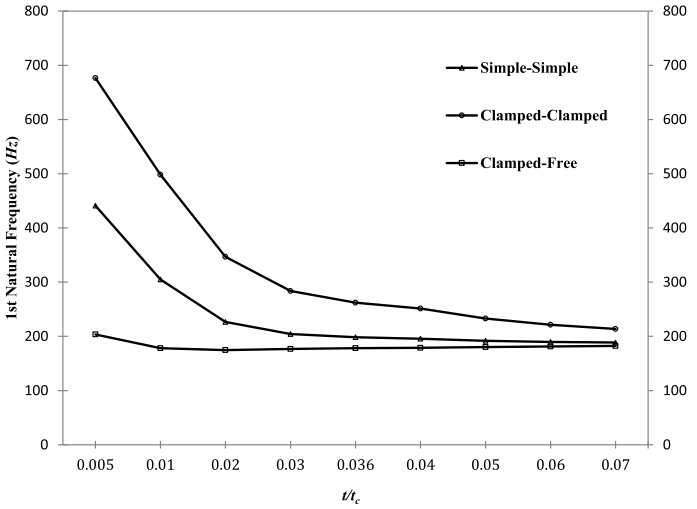


**Figure 6.** Variation in first natural frequency with $t/t_c$.

**Table 5.** Natural frequencies (Hz) of the frame in Example 4

| Freq. No. | Length of the straight beam (m) | | | | | | Results of Example 2 |
|---|---|---|---|---|---|---|---|
| | 0.4 | | 0.2 | | 0.05 | 0.001 | |
| | Current theory | ABAQUS | Current theory | ABAQUS | | | |
| 1 | 194.352 | 196.7056 | 214.1217 | 209.8393 | 245.6083 | 261.6727 | 262.0415 |
| 2 | 282.9247 | 286.3509 | 362.4141 | 355.1658 | 466.8177 | 514.4214 | 515.4826 |
| 3 | 446.6675 | 452.0766 | 601.0842 | 589.0625 | 787.8813 | 869.6252 | 871.4298 |
| 4 | 660.2134 | 668.2086 | 892.072 | 874.2306 | 1161.8662 | 1277.6902 | 1280.2359 |
| 5 | 905.7481 | 916.7167 | 1214.7961 | 1190.5 | 1566.4927 | 1715.7687 | 1719.0399 |

**Table 6.** Natural frequencies (Hz) of simply supported curved sandwich beam

| Mode | Face/core thickness ratio | | | | | | | | |
|---|---|---|---|---|---|---|---|---|---|
| | $t/t_c = 0.005$ | $t/t_c = 0.01$ | $t/t_c = 0.02$ | $t/t_c = 0.03$ | $t/t_c = 0.036$ | $t/t_c = 0.04$ | $t/t_c = 0.05$ | $t/t_c = 0.06$ | $t/t_c = 0.07$ |
| 1 | 441.1567 | 305.0456 | 226.5296 | 204.3470 | 198.3981 | 195.7702 | 191.8288 | 189.8133 | 188.7099 |
| 2 | 1269.1684 | 896.9036 | 580.0264 | 442.3579 | 392.9364 | 367.7215 | 322.1543 | 292.1560 | 271.3317 |
| 3 | 2166.6490 | 1625.2373 | 1100.7168 | 843.1455 | 743.4269 | 690.5363 | 590.1485 | 519.5161 | 467.4218 |
| 4 | 3055.9792 | 2376.5712 | 1680.0883 | 1316.2752 | 1169.8081 | 1090.5666 | 936.5129 | 824.6754 | 739.8788 |
| 5 | 3931.2771 | 3123.6820 | 2275.9073 | 1818.8453 | 1630.6193 | 1527.5399 | 1324.1196 | 1173.5140 | 1057.3412 |
| 6 | 6505.9800 | 3861.9549 | 2872.6895 | 2331.1017 | 2105.1944 | 1980.5930 | 1732.3224 | 1546.1203 | 1400.8007 |
| 7 | 7356.2522 | 4592.0975 | 3465.4645 | 2844.4591 | 2583.6794 | 2439.2250 | 2149.7367 | 1930.8139 | 1758.6082 |

frequency of the simply supported and the clamped–clamped curved sandwich beams decreases, while the first natural frequency of the cantilever beam initially decreases and then increases slightly. This is because bending stiffness is affected due to the variation in the thickness of layers.

The natural frequency variation with radius/length ratios is shown in Tables 9–11. In this case, the beam length is considered constant, but the beam radius is varied. The ratio of the radius to the length of the studied beam in Table 1 is $R/L = 6$. Finally, the first natural frequency variation with $R/L$ ratios is shown in Figure 7. As is obvious in Figure 7, regardless of the boundary condition type, when the radius/length ratio is increased, the natural frequencies decrease. This

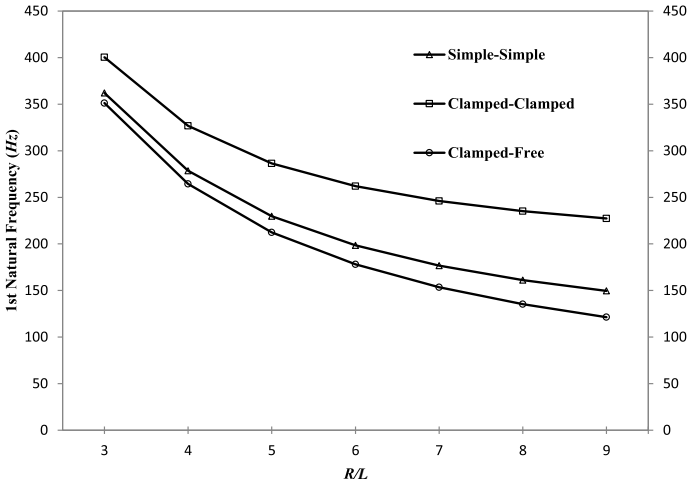


**Figure 7.** Variation in first natural frequency with $R/L$.

**Table 7.** Natural frequencies (Hz) of clamped–clamped curved sandwich beam

| Mode | Face/core thickness ratio | | | | | | | | |
|---|---|---|---|---|---|---|---|---|---|
| | $t/t_c = 0.005$ | $t/t_c = 0.01$ | $t/t_c = 0.02$ | $t/t_c = 0.03$ | $t/t_c = 0.036$ | $t/t_c = 0.04$ | $t/t_c = 0.05$ | $t/t_c = 0.06$ | $t/t_c = 0.07$ |
| 1 | 676.5804 | 498.1699 | 346.6145 | 283.5876 | 262.0415 | 251.3821 | 232.8582 | 221.3132 | 213.6784 |
| 2 | 1393.3100 | 1062.0884 | 738.3015 | 577.7566 | 515.4826 | 482.4824 | 420.0601 | 376.4699 | 344.6312 |
| 3 | 2225.1003 | 1730.1208 | 1233.2649 | 975.3312 | 871.4298 | 815.1661 | 705.6735 | 626.1120 | 565.7858 |
| 4 | 3078.9171 | 2437.0599 | 1775.9446 | 1424.3711 | 1280.2359 | 1201.3941 | 1045.8973 | 930.7671 | 841.9129 |
| 5 | 6516.6326 | 3160.1721 | 2343.0952 | 1901.8418 | 1719.0399 | 1618.4659 | 1418.5846 | 1268.9949 | 1152.3633 |
| 6 | 7348.9513 | 3885.2600 | 2920.5603 | 2394.0886 | 2174.4006 | 2053.0771 | 1810.7129 | 1628.0549 | 1484.6967 |
| 7 | 7995.3571 | 4608.7714 | 3501.1267 | 2893.1264 | 2638.2352 | 2497.0890 | 2214.1503 | 1999.8777 | 1830.9360 |

**Table 8.** Natural frequencies (Hz) of cantilever curved sandwich beam

| Mode | Face/core thickness ratio | | | | | | | | |
|---|---|---|---|---|---|---|---|---|---|
| | $t/t_c = 0.005$ | $t/t_c = 0.01$ | $t/t_c = 0.02$ | $t/t_c = 0.03$ | $t/t_c = 0.036$ | $t/t_c = 0.04$ | $t/t_c = 0.05$ | $t/t_c = 0.06$ | $t/t_c = 0.07$ |
| 1 | 203.5314 | 178.1010 | 174.6543 | 176.7994 | 178.0778 | 178.7587 | 180.2606 | 181.4085 | 182.3038 |
| 2 | 742.7778 | 529.3031 | 356.7094 | 287.7490 | 264.6783 | 253.2926 | 233.7711 | 221.7394 | 213.8516 |
| 3 | 1600.0192 | 1182.7375 | 794.8032 | 610.3972 | 540.3804 | 503.5813 | 434.7018 | 387.1439 | 352.7017 |
| 4 | 2476.4789 | 1906.5706 | 1331.6039 | 1038.3522 | 921.8040 | 859.0934 | 738.0510 | 650.9510 | 585.4255 |
| 5 | 3362.6367 | 2654.3428 | 1911.0955 | 1517.5808 | 1357.3238 | 1269.9910 | 1098.6723 | 972.7112 | 876.0916 |
| 6 | 6688.2504 | 3398.8743 | 2504.6669 | 2019.8048 | 1819.2553 | 1709.1274 | 1490.7946 | 1328.0522 | 1201.6687 |
| 7 | 7141.4991 | 4137.1116 | 3100.4683 | 2530.9081 | 2293.0884 | 2161.7918 | 1899.7375 | 1702.5968 | 1548.2029 |

is because of the decrease in bending stiffness with increasing radius of the curved beam. The natural frequencies of a straight beam with the same properties listed in Table 1 except that $R = \infty$ are presented in the last column. As can be seen in Tables 9–11, at upper frequencies, with variation in the radius/length ratio, the differences between frequencies decrease. Therefore, the tenth frequencies for different radius/length ratios are very close together, and it can be concluded that the effect of curvature on upper frequencies is less.

**Table 9.** Natural frequencies (Hz) of simply supported curved sandwich beam

| Mode | Radius/length ratio | | | | | | | |
|---|---|---|---|---|---|---|---|---|
| | $R/L=3$ | $R/L=4$ | $R/L=5$ | $R/L=6$ | $R/L=7$ | $R/L=8$ | $R/L=9$ | $R=\infty$ |
| 1 | 362.0003 | 278.5001 | 229.7919 | 198.3981 | 176.7544 | 161.1729 | 149.5535 | 93.5720 |
| 2 | 496.5171 | 439.1168 | 409.7832 | 392.9364 | 382.3430 | 375.3223 | 370.4220 | 351.0407 |
| 3 | 803.9435 | 769.3234 | 752.6597 | 743.4269 | 737.7204 | 733.9912 | 731.4085 | 721.0534 |
| 4 | 1210.1645 | 1186.9369 | 1175.8964 | 1169.8081 | 1166.0356 | 1163.5686 | 1161.8545 | 1154.6642 |
| 5 | 1660.6365 | 1643.3661 | 1635.1577 | 1630.6193 | 1627.7923 | 1625.9359 | 1624.6395 | 1618.9420 |
| 6 | 2129.1663 | 2115.4108 | 2108.8528 | 2105.1944 | 2102.9307 | 2101.4287 | 2100.3736 | 2095.5507 |
| 7 | 2603.6915 | 2592.2330 | 2586.7504 | 2583.6794 | 2581.7727 | 2580.5000 | 2579.6035 | 2575.3767 |
| 8 | 3078.8213 | 3068.9839 | 3064.2613 | 3061.6066 | 3059.9527 | 3058.8451 | 3058.0623 | 3054.2829 |
| 9 | 3552.3002 | 3543.6736 | 3539.5203 | 3537.1787 | 3535.7158 | 3534.7335 | 3534.0374 | 3530.6142 |
| 10 | 4023.3316 | 4015.6486 | 4011.9403 | 4009.8447 | 4008.5312 | 4007.6492 | 4007.0221 | 4003.8931 |

**Table 10.** Natural frequencies (Hz) of clamped–clamped curved sandwich beam

| Mode | Radius/length ratio | | | | | | | |
|---|---|---|---|---|---|---|---|---|
| | $R/L=3$ | $R/L=4$ | $R/L=5$ | $R/L=6$ | $R/L=7$ | $R/L=8$ | $R/L=9$ | $R=\infty$ |
| 1 | 400.3792 | 326.8695 | 286.5300 | 262.0415 | 246.0767 | 235.1449 | 227.3470 | 195.2168 |
| 2 | 597.6979 | 551.2195 | 528.3241 | 515.4826 | 507.5457 | 502.3447 | 498.7463 | 484.9597 |
| 3 | 922.3984 | 893.0089 | 879.0732 | 871.4298 | 866.7558 | 863.7225 | 861.6364 | 853.7371 |
| 4 | 1315.4372 | 1295.0094 | 1285.4443 | 1280.2359 | 1277.0572 | 1275.0012 | 1273.5897 | 1268.2617 |
| 5 | 1745.4078 | 1730.0670 | 1722.9202 | 1719.0399 | 1716.6731 | 1715.1442 | 1714.0954 | 1710.1410 |
| 6 | 2195.3194 | 2183.1411 | 2177.4812 | 2174.4006 | 2172.5393 | 2171.3331 | 2170.5046 | 2167.3827 |
| 7 | 2655.5078 | 2645.4458 | 2640.7755 | 2638.2352 | 2636.7020 | 2635.7068 | 2635.0241 | 2632.4524 |
| 8 | 3120.3565 | 3111.7943 | 3107.8233 | 3105.6640 | 3104.3613 | 3103.5155 | 3102.9356 | 3100.7510 |
| 9 | 3586.7354 | 3579.2855 | 3575.8319 | 3573.9546 | 3572.8221 | 3572.0869 | 3571.5827 | 3569.6841 |
| 10 | 4052.9878 | 4046.3930 | 4043.3368 | 4041.6758 | 4040.6727 | 4040.0235 | 4039.5775 | 4037.8981 |

**Table 11.** Natural frequencies (Hz) of cantilever curved sandwich beam

| Mode | Radius/length ratio | | | | | | | |
|---|---|---|---|---|---|---|---|---|
| | $R/L=3$ | $R/L=4$ | $R/L=5$ | $R/L=6$ | $R/L=7$ | $R/L=8$ | $R/L=9$ | $R=\infty$ |
| 1 | 351.2354 | 264.3706 | 212.4634 | 178.0778 | 153.5863 | 135.3773 | 121.3244 | 33.7455 |
| 2 | 401.9126 | 328.8635 | 288.8645 | 264.6783 | 248.8537 | 238.0653 | 230.3777 | 198.7873 |
| 3 | 619.1296 | 574.4774 | 552.5895 | 540.3804 | 532.7970 | 527.8545 | 524.4377 | 511.3698 |
| 4 | 970.0016 | 942.1611 | 928.9925 | 921.8040 | 917.3714 | 914.5126 | 912.5470 | 905.1088 |
| 5 | 1390.4815 | 1371.2149 | 1362.2050 | 1357.3238 | 1354.3105 | 1352.3765 | 1351.0488 | 1346.0384 |
| 6 | 1844.1536 | 1829.6707 | 1822.9283 | 1819.2553 | 1817.0372 | 1815.5957 | 1814.6070 | 1810.8797 |
| 7 | 2312.8974 | 2301.3629 | 2296.0044 | 2293.0884 | 2291.3272 | 2290.1853 | 2289.4013 | 2286.4473 |
| 8 | 2787.3462 | 2777.7780 | 2773.3381 | 2770.9234 | 2769.4659 | 2768.5202 | 2767.8714 | 2765.4274 |
| 9 | 3262.8311 | 3254.6566 | 3250.8661 | 3248.8051 | 3247.5616 | 3246.7546 | 3246.2007 | 3244.1163 |
| 10 | 3737.1438 | 3730.0049 | 3726.6960 | 3724.8973 | 3723.8124 | 3723.1080 | 3722.6250 | 3720.8062 |

## 6. Conclusions

First, assuming the face layers to behave like Euler–Bernoulli beams while only shear deformation occurs in the core, by employing the Hamilton principle, the differential equations of motion of a symmetric curved sandwich beam are formulated and applied to obtain the dynamic stiffness matrix for this beam. By assembling the element matrices in a common procedure, the dynamic stiffness matrix for the overall structure can be produced. Then, to calculate the natural frequencies, the Wittrick–Williams algorithm is applied to this dynamic stiffness matrix. The results of the current study agree well with the available results of other theories. The present formulation has the advantage over other theories that it also enables computing the natural frequencies of a complex frame consisting of curved and straight sandwich members to study the

dynamic behavior of complex sandwich frames to estimate the resonance frequency. Reduction in the natural frequencies of the curved sandwich beam with increasing face/core thickness and radius/length ratios regardless of the boundary condition type is demonstrated through parametric studies.

## References


[1] A. A. Khdeir, O. J. Aldraihem, "Free vibration of sandwich beams with soft core", *Compos. Struct.* **154** (2016), p. 179-189.

[2] R. A. Di Taranto, "Theory of vibratory bending for elastic and viscoelastic layered finite length beams", *J. Appl. Mech.* **32** (1965), p. 881-886.

[3] D. J. Mead, S. Sivakumaran, "The Stodola method applied to sandwich beam vibration", in *Proceedings of the Symposium on Numerical Methods for Vibration Problems*, University of Southampton, Institute of Sound and Vibration Research, 1967, p. 66-80.

[4] D. J. Mead, S. Markus, "The forced vibration of a three-layer damped sandwich beam with arbitrary boundary conditions", *J. Sound Vib.* **10** (1969), p. 163-175.

[5] K. M. Ahmed, "Free vibration of curved sandwich beams by the method of finite elements", *J. Sound Vib.* **18** (1971), p. 61-74.

[6] K. M. Ahmed, "Static and dynamic analysis of sandwich structures by the method of finite element", *J. Sound Vib.* **18** (1971), p. 75-91.

[7] T. Sakiyama, H. Matsuda, C. Morita, "Free vibration analysis of sandwich arches with elastic or visco elastic core and various kinds of axis shape and boundary conditions", *J. Sound Vib.* **203** (1997), p. 505-522.

[8] S. R. Marur, T. Kant, "Free vibration of higher-order sandwich and composite arches, Part I: Formulation", *J. Sound Vib.* **310** (2008), p. 91-109.

[9] M. C. Amirani, S. M. R. Khalili, N. Nemati, "Free vibration analysis of sandwich beam with FG core using the element free Galerkin method", *Compos. Struct.* **90** (2009), p. 373-379.

[10] S. M. Hashemi, E. J. Adique, "Free vibration analysis of sandwich beams: A dynamic finite element", *Int. J. Vehicle Struct. Sys.* **1** (2009), p. 59-65.

[11] S. M. Hashemi, E. J. Adique, "A quasi-exact dynamic finite element for free vibration analysis of sandwich beams", *Appl. Compos. Mater.* **17** (2010), p. 259-269.

[12] H. Arvin, M. Sadighi, A. R. Ohadi, "A numerical study of free and forced vibration of composite sandwich beam with viscoelastic core", *Compos. Struct.* **92** (2010), p. 996-1008.

[13] S. M. R. Khalili, N. Nemati, K. Malekzadeh, A. R. Damanpack, "Free vibration analysis of sandwich beams using improved dynamic stiffness method", *Compos. Struct.* **92** (2010), p. 387-394.

[14] E. Sadeghpour, M. Sadighi, A. Ohadi, "Free vibration analysis of a debonded curved sandwich beam", *Europ. J. Mech./A Solids* **57** (2016), p. 71-84.

[15] D. Chen, S. Kitipornchai, J. Yang, "Nonlinear free vibration of shear deformable sandwich beam with a functionally graded porous core", *Thin-Walled Struct.* **107** (2016), p. 39-48.

[16] J. R. Banerjee, "Dynamic stiffness formulation for structural elements: A general approach", *Comput. Struct.* **63** (1997), p. 101-103.

[17] J. R. Banerjee, "Free vibration of sandwich beams using the dynamic stiffness method", *Comput. Struct.* **81** (2003), p. 1915-1922.

[18] J. R. Banerjee, "Development of an exact dynamic stiffness matrix for free vibration analysis of a twisted Timoshenko beam", *J. Sound Vib.* **270** (2004), p. 379-401.

[19] J. R. Banerjee, A. J. Sobey, "Dynamic stiffness formulation and free vibration analysis of a three-layered sandwich beam", *Int. J. Solids Struct.* **42** (2005), p. 2181-2197.

[20] W. P. Howson, A. Zare, "Exact dynamic stiffness matrix for flexural vibration of three-layered sandwich beams", *J. Sound Vib.* **282** (2005), p. 753-767.

[21] J. R. Banerjee, C. W. Cheung, R. Morishima, M. Perera, J. Njuguna, "Free vibration of a three-layered sandwich beam using the dynamic stiffness method and experiment", *Int. J. Solids Struct.* **44** (2007), p. 7543-7563.

[22] J. R. Banerjee, "Gunawardana W.D. Dynamic stiffness matrix development and free vibration analysis of a moving beam", *J. Sound Vib.* **303** (2007), p. 135-143.

[23] A. R. Damanpack, S. M. R. Khalili, "High-order free vibration analysis of sandwich beams with a flexible core using dynamic stiffness method", *Compos. Struct.* **94** (2012), p. 1503-1514.

[24] W. H. Wittrick, F. W. Williams, "A general algorithm for computing natural frequencies of elastic structures", *Q. J. Mech Appl. Math.* **24** (1971), p. 263-284.

[25] H. Su, J. R. Banerjee, C. W. Cheung, "Dynamic stiffness formulation and free vibration analysis of functionally graded beams", *Compos. Struct.* **106** (2013), p. 854-862.

[26] A. Pagani, E. Carrera, M. Boscolo, J. R. Banerjee, "Refined dynamic stiffness elements applied to free vibration analysis of generally laminated composite beams with arbitrary boundary conditions", *Compos. Struct.* **110** (2014), p. 305-316.
[27] J. R. Banerjee, D. R. Jackson, "Free vibration of a rotating tapered Rayleigh beam: A dynamic stiffness method of solution", *Comput. Struct.* **124** (2013), p. 11-20.
[28] J. R. Banerjee, D. Kennedy, "Dynamic stiffness method for inplane free vibration of rotating beams including Coriolis effects", *J. Sound Vib.* **333** (2014), p. 7299-7312.
[29] H. Su, J. R. Banerjee, "Development of dynamic stiffness method for free vibration of functionally graded Timoshenko beams", *Comput. Struct.* **147** (2015), p. 107-116.
[30] A. Zare, B. Rafezy, W. P. Howson, "Coupled bending-longitudinal vibration of three layer sandwich beam using exact dynamic stiffness matrix", *J. Solid Mech.* **9** (2017), p. 730-750.
[31] F. W. Williams, W. H. Wittrick, "Exact buckling and frequency calculations surveyed", *J. Struct. Eng.* **109** (1983), p. 169-187.
[32] F. W. Williams, "Review of exact buckling and frequency calculations with optional multi-level substructuring", *Comput. Struct.* **48** (1993), p. 547-552.
[33] E. Adique, "Free vibration analysis of sandwich beams using dynamic finite element (DFE) and FEM formulations", MSc Thesis, Ryerson University, Canada, 2008.
[34] K. M. Ahmed, "Dynamic analysis of sandwich beams", *J. Sound Vib.* **21** (1972), p. 263-276.